

New Design of Mems piezoresistive pressure sensor

Hamsa Kamali, Asghar Charmin

Department of Electrical Engineering, Islamic Azad University, Ahar Branch, Ahar, Iran

Email :hams.kamali@gmail.com

Abstract

The electromechanical analysis of a piezoresistive pressure microsensor with a square-shaped diaphragm for low-pressure biomedical applications is presented. This analysis is developed through a novel model and a finite element method (FEM) model. A microsensor with a diaphragm 1000 μm length and with thickness=400 μm is studied. The electric response of this microsensor is obtained with applying voltage into sensor in p-type piezoresistors located on the diaphragm surface. The diaphragm that is 10 μm thick exhibits a maximum deflection of 3.74 μm using the designed model, which has a relative difference of 5.14 and 0.92% with respect to the comsol model, respectively. The maximum sensitivity and normal stress calculated using the this model are 1.64 mV/V/kPa and 102.1 MPa, respectively. The results of the polynomial model agree well with the Timoshenko model and FEM model for small deflections. In addition, the designed model can be easily used to predict the deflection, normal stress, electric response and sensitivity of a piezoresistive pressure microsensor with a square-shaped diaphragm under small deflections.

Keywords: Finite element model; piezoresistors; Crystal ; pressure microsensor.

1- Introduction

Piezoresistive pressure sensors were some of the first MEMS devices to be commercialized. Compared to capacitive pressure sensors, they are simpler to integrate with electronics, their response is more linear, and they are inherently shielded from RF noise. They do, however, usually require more power during operation, and the fundamental noise limits of the sensor are higher than their capacitive counterparts. Historically, piezoresistive devices have been dominant in the pressure sensor market.

Although the sensor is no longer in production, a detailed analysis of its design is given in [1], and an archived data sheet is

available from Free scale Semiconductor Inc.[2]

The model consists square membrane with side 1 mm and thickness 20 μm , supported around its edges by region 0.1mm wide, which is intended to represent the remainder of the wafer. The supporting region is fixed on its underside (representing a connection to the thicker handle of the device die). Near to one edge of the membrane an X-shaped

piezoresistor (or X_{ducer}) and part of its associated interconnects are visible. The geometry is shown in Figure 1.

The piezoresistor is assumed to have a uniform p-type dopant density of $1.32 \cdot 10^{19} \text{ cm}^{-3}$ and a thickness of 400 nm.

The interconnects are assumed to have the same thickness but a dopant density of $.45 \cdot 10^{20} \text{ cm}^{-3}$. Only a part of the interconnects is included in the geometry, since their conductivity is sufficiently high that they do not contribute to the voltage output of the device (in practice the interconnects would also be thicker in addition to having a higher conductivity but this also has little effect on the solution).

The edges of the die are aligned with the $\{110\}$ directions of the silicon. The die edges are also aligned with the global X and Y axes in the COMSOL model. The piezoresistor is oriented at 45° to the die edge, and so lies in the $[100]$ direction of the crystal. In the COMSOL model, a coordinate system rotated 45° about the global Z -axis is added to define the orientation of the crystal.

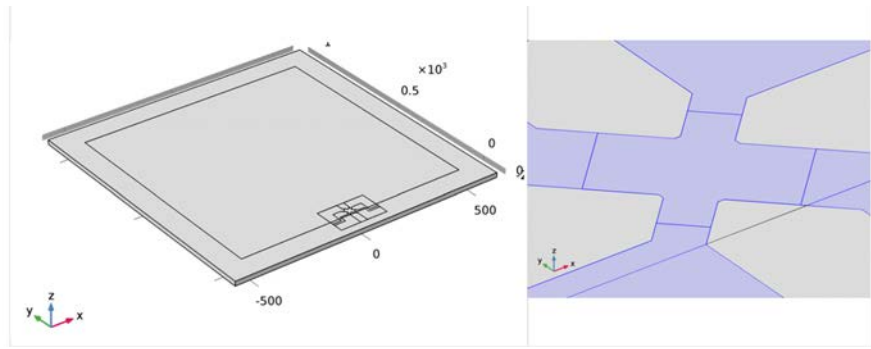


Fig.1.Left: Model geometry. Right: Detail showing the piezoresistor geometry.

2- Device Physics and Equations

The conductivity of the $X_{\text{ducer}}^{\text{TM}}$ sensor changes when the membrane in its vicinity is subject to an applied stress. This effect is known as the piezoresistance effect and is usually associated with semiconducting materials. In semiconductors, piezoresistance results from the strain-induced alteration of the material's band structure, and the associated changes in carrier mobility and number density. The relation between the electric field, E , and the current, J , within a piezoresistor is:

$$E = \rho \cdot J + \Delta\rho \cdot J \quad (1)$$

where ρ is the resistivity and $\Delta\rho$ is the induced change in the resistivity. In the general case both ρ and $\Delta\rho$ are rank 2 tensors (matrices). The change in resistance is related to the stress, σ , by the constitutive relationship:

$$\Delta\rho = \Pi \sigma \quad (2)$$

where Π is the piezoresistance tensor (SI units: $\text{Pa}^{-1}\Omega\text{m}$), a material property. Note that our definition of Π includes the resistivity in each element of the tensor, rather than having a scalar multiple outside of Π (which is possible only for materials

with isotropic conductivity). Π is in this case a rank-4 tensor; however, it can be represented as a matrix if the resistivity and stress are converted to vectors within a reduced subscript notation. Within the Voigt notation :

$$\begin{bmatrix} \Delta\rho_{xx} \\ \Delta\rho_{yy} \\ \Delta\rho_{zz} \\ \Delta\rho_{yz} \\ \Delta\rho_{xz} \\ \Delta\rho_{xy} \end{bmatrix} = \begin{bmatrix} \Pi_{11} & \Pi_{12} & \Pi_{13} & \Pi_{14} & \Pi_{15} & \Pi_{16} \\ \Pi_{21} & \Pi_{22} & \Pi_{23} & \Pi_{24} & \Pi_{25} & \Pi_{26} \\ \Pi_{31} & \Pi_{32} & \Pi_{33} & \Pi_{34} & \Pi_{35} & \Pi_{36} \\ \Pi_{41} & \Pi_{42} & \Pi_{43} & \Pi_{44} & \Pi_{45} & \Pi_{46} \\ \Pi_{51} & \Pi_{52} & \Pi_{53} & \Pi_{54} & \Pi_{55} & \Pi_{56} \\ \Pi_{61} & \Pi_{62} & \Pi_{63} & \Pi_{64} & \Pi_{65} & \Pi_{66} \end{bmatrix} \cdot \begin{bmatrix} \sigma^{xx} \\ \sigma^{yy} \\ \sigma^{zz} \\ \sigma^{yz} \\ \sigma^{xz} \\ \sigma^{xy} \end{bmatrix}$$

The $\Delta\rho$ vector computed from Equation 3 is assembled into matrix form in the following manner in Equation 1:

$$\begin{bmatrix} E_x \\ E_y \\ E_z \end{bmatrix} = \begin{bmatrix} \rho_{xx} & \rho_{xy} & \rho_{xz} \\ \rho_{xy} & \rho_{yy} & \rho_{yz} \\ \rho_{xz} & \rho_{yz} & \rho_{zz} \end{bmatrix} \cdot \begin{bmatrix} J_x \\ J_y \\ J_z \end{bmatrix} + \begin{bmatrix} \Delta\rho_{xx} & \Delta\rho_{xy} & \Delta\rho_{xz} \\ \Delta\rho_{xy} & \Delta\rho_{yy} & \Delta\rho_{yz} \\ \Delta\rho_{xz} & \Delta\rho_{yz} & \Delta\rho_{zz} \end{bmatrix} \cdot \begin{bmatrix} J_x \\ J_y \\ J_z \end{bmatrix}$$

Silicon has cubic symmetry, and as a result the Π matrix can be described in terms of three independent constants in the following manner:

$$\Pi = \begin{bmatrix} \Pi_{11} & \Pi_{12} & \Pi_{12} & 0 & 0 & 0 \\ \Pi_{12} & \Pi_{22} & \Pi_{12} & 0 & 0 & 0 \\ 0 & 0 & 0 & \Pi_{44} & 0 & 0 \\ 0 & 0 & 0 & 0 & \Pi_{44} & 0 \\ 0 & 0 & 0 & 0 & 0 & \Pi_{44} \end{bmatrix}$$

For p-type silicon the Π_{44} constant is two orders of magnitude larger than either the Π_{11} or the Π_{12} coefficients. The Π_{66} element (which is equal in magnitude to the Π_{44} element) couples the σ_{xy} shear stress, with the $\Delta\rho_{xy}$ off-diagonal term in the change in resistivity matrix. In turn, $\Delta\rho_{xy}$ couples a

current in the x -direction to an induced electric field in the y -direction (and vice versa).

This is the principle of the Xducer transducer. An applied voltage (typically 3 V; see [2]) across the [100] orientated arm of the X produces a current (typically 6 mA; see [2]) down this arm. Shear stresses are present in the XducerTM as a result of the pressure induced deformation of the diaphragm in which it is implanted. Through the piezoresistance effect, these shear stresses cause an electric field or potential gradient transverse to the direction of current flow, in the [010] arm of the X.

Across the width of the transducer, the potential gradient sums up to produce an induced voltage difference between the [010] arms of the X. According to the device data sheet, under normal operating conditions a 60 mV potential difference is generated from a 100 kPa applied pressure with a 3 V applied bias [2].

The situation is complicated somewhat by the detailed current distribution within the device, since the voltage sensing elements increase the width of the current carrying silicon wire locally, leading to a ‘‘short circuit’’ effect [3] or a spreading out of the current into the sense arms of the X.

Our Piezoresistivity interfaces solve Equation 3 and an inverse form of Equation 4, together with the equations of structural mechanics. In this model the *Piezoresistivity*, *Boundary Currents* interface is used to model the structural equations on the domain level and to solve the electrical equations on a thin layer coincident with a boundary in the model geometry.

3- Results and Discussion

Figure 2 shows the displacement of the diaphragm as a result of a 100 kPa pressure difference. At the center of the diaphragm the displacement is $1.2 \mu\text{m}$. A simple isotropic model for the deform displacement given in [1] predicts an order of magnitude value of $4 \mu\text{m}$ (assuming a Young's modulus of 170 GPa and a Poisson's ratio of 0.06). The agreement is reasonable considering the limitations of the analytic model, which is derived by a crude variational guess. A more accurate value for the shear stress in local coordinates at the midpoint of the diaphragm edge is given in [1] as:

$$\sigma^{1,2} = 0.141 \left(\frac{L}{H}\right)^2 P \quad (3)$$

where P is the applied pressure, L is the length of the diaphragm edge, and H is the diaphragm thickness. This equation predicts the magnitude of the local shear stress to be 35 MPa, in good agreement with the minimum value shown in Figure 3, which is also 35 MPa. Theoretically the shear stress should be maximal at the midpoint of the edge of the diaphragm. Figure 4 shows the shear stress along the edge in the model. This shows a maximum magnitude at the center of each of the two edges along which the plot is made, but the value of this maximum is less than the maximum stress in the model, in part due to the boundary conditions employed on the three dimensional diaphragm. The model: Piezoresistive_pressure_sensor_shell.mph shows better agreement with the theoretical maximum shear stress along this edge.

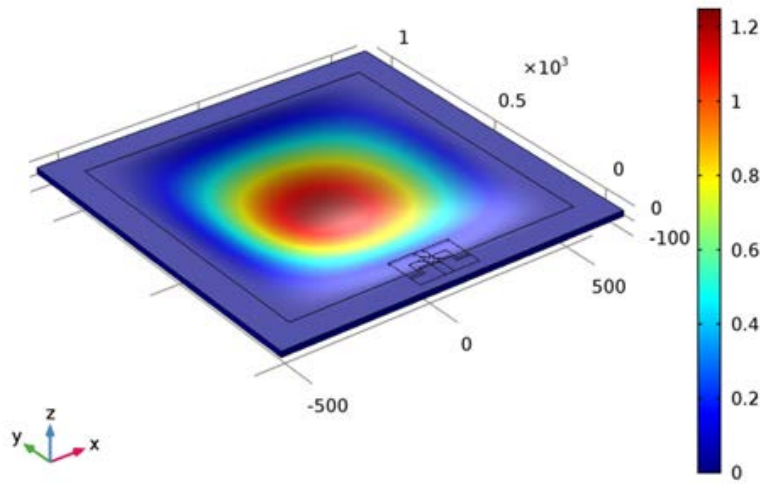


Fig.2. Diaphragm displacement as a result of a 100 kPa applied pressure.

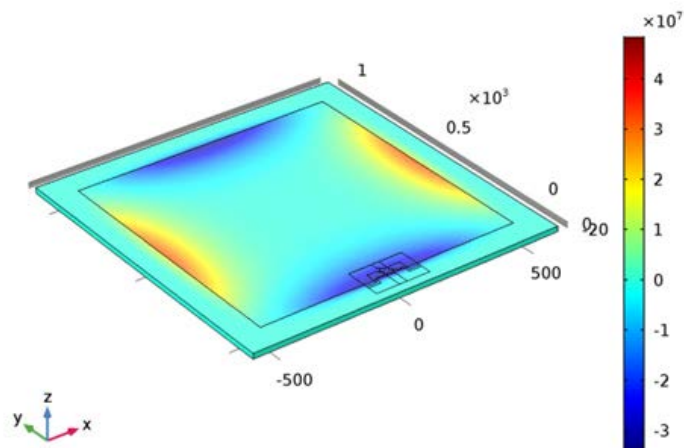


Fig.3. Shear stress, shown in the local co-ordinate system of the piezoresistor (rotated 45° about the z-axis of the global system).

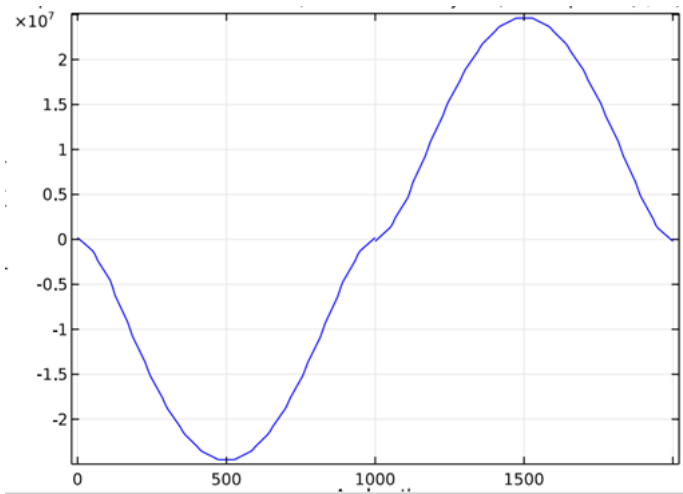


Fig.4. Plot of the local shear stress along two edges of the diaphragm.

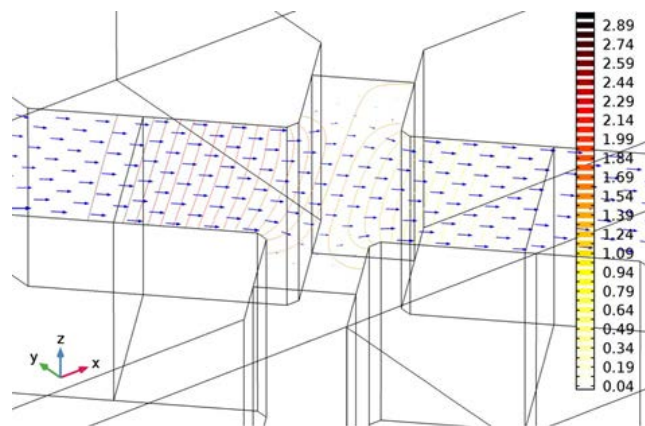


Fig.5. Arrows: Current density, Contours: Electric Potential, for a device driven by a 3 V bias with an applied pressure of 100 kPa.

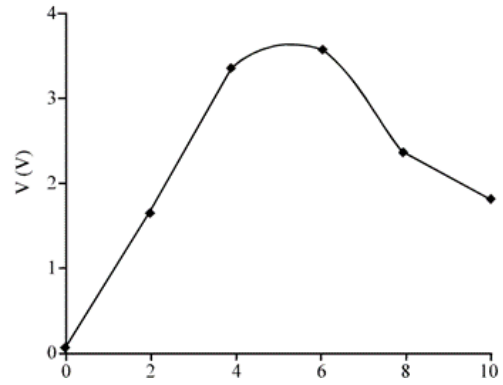


Fig.6. Output Voltage vs pressure modified sensor

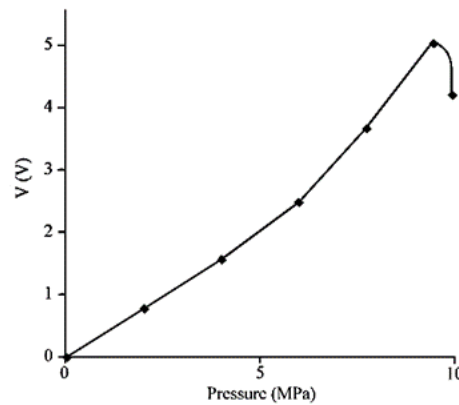


Fig.7. Output Voltage vs pressure modified sensor

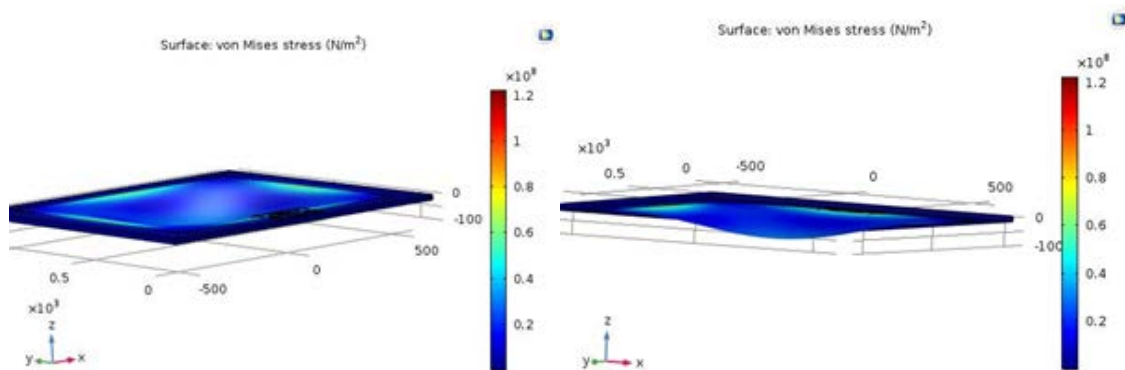


Fig.8. Deformation of sensor on applying Pressure

The output of the model during normal operation shows good agreement with the manufacturer's data sheet, given that the device dimensions and doping levels have

been guessed. With an applied bias of 3 V a typical operating current of 5.9 mA is obtained (compare the current quoted in [2] of 6 mA). The model produces an output

voltage of 52 mV, similar to the actual device output of 60 mV quoted in [2]. The detailed current and voltage distribution within the Xducer is shown in [5]. There is clear evidence of the current flow “spreading out” into the sense electrodes (which are narrower), a phenomena described in [3] as the “short circuit” effect. The asymmetry in the potential, which is induced by the piezoresistive effect, is also apparent in the figure.

References

- [1] Senturia, S. D. "Chapter 18:“A Piezoresistive Pressure Sensor”, *Microsystem Design*." (2000).
- [2] Motorola Semiconductor MPX100 series technical data, document: MPX100/D, 1998 (available from Freescale Semiconductor Inc at <http://www.freescale.com>).
- [3] Bao, Minhang. *Analysis and design principles of MEMS devices*. Elsevier, 2005.
- [4] Beeby, Stephen, et al. *MEMS mechanical sensors*. Artech House, 2004.
- [5] H.P. Le, K. Shah, J. Singh, and A. Zayegh, *Analog Integr. Circ.Sig. Process.* **48** (2006) 21.
- [6] Le, Hai Phuong, et al. "Design and implementation of an optimised wireless pressure sensor for biomedical application." *Analog Integrated Circuits and Signal Processing* 48.1 (2006): 21-31.
- [7] Lin, Liwei, and Weijie Yun. "Design, optimization and fabrication of surface micromachined pressure sensors." *Mechatronics* 8.5 (1998): 505-519.
- [8] Lin, Liwei, Huey-Chi Chu, and Yen-Wen Lu. "A simulation program for the sensitivity and linearity of piezoresistive pressure sensors." *Journal of microelectromechanical systems* 8.4 (1999): 514-522.
- [9] Bistue, G., et al. "A design tool for pressure microsensors based on FEM simulations." *Sensors and Actuators A: Physical* 62.1-3 (1997): 591-594.
- [10] Herrera-May, A. L., et al. "Electromechanical analysis of a piezoresistive pressure microsensor for low-pressure biomedical applications." *Revista mexicana de física* 55.1 (2009): 14-24.
- [11] A.C. Ugural, *Stresses in Plates and Shells* (New York: McGrawHill, 1981).